On the Determination of the Optimal Scan Mode Sequence for the TRMM CERES Instrument

TAKMENG WONG AND EDWIN F. HARRISON

NASA/Langley Research Center, Hampton, Virginia

GARY G. GIBSON AND FREDERICK M. DENN

Analytical Services and Materials, Inc., Hampton, Virginia

17 July 1996 and 27 February 1997

ABSTRACT

Clouds and the Earth's Radiant Energy System (CERES) is a NASA spaceborne measurement program for monitoring the radiation environment of the earth–atmosphere system. The first CERES instrument is scheduled to be launched on board the Tropical Rainfall Measuring Mission (TRMM) satellite in late 1997. In addition to gathering traditional cross-track fixed azimuth measurements for calculating monthly mean radiation fields, this single CERES scanner instrument will also be required to collect angular radiance data using a rotating azimuth configuration for developing new angular dependence models (ADMs). Since the TRMM single CERES instrument can only be run in either one of these two configurations at any one time, it will need to be operated in a cyclical pattern between these two scan modes to achieve the intended measurement goals. To minimize the errors in the derived monthly mean radiation field due to missing cross-track scanner measurements during this satellite mission, determination of the optimal scan mode sequence for the TRMM single CERES instrument is carried out. The Earth Radiation Budget Experiment S-4 daily mean cross-track scanner data product for April and July 1985 and January 1986 is used with a simple temporal sampling scheme to produce simulated daily mean cross-track scanner measurements under different TRMM CERES operational scan mode sequences. Error analysis is performed on the monthly mean radiation fields derived from these simulated datasets. It is found that the best monthly mean result occurred when the cross-track scanner is operated on a ''2 days on and 1 day off'' mode. This scan mode sequence will effectively allow for 2 consecutive days of cross-track scanner data and 1 day of angular radiance measurement for each 3-day period. The root-mean-square errors for the monthly mean all-sky (clear sky) longwave and shortwave radiation field, due to missing cross-track scanner measurements for this particular case, are expected to be less than 2.5 (0.5) and 5.0 (1.5) W m^{-2}, respectively.

1. Introduction

Continuous monitoring of the earth's radiation fields at the top of the atmosphere (TOA) is essential to understanding the earth's climate and climate change. To achieve this science goal, NASA has begun the Clouds and the Earth's Radiant Energy System (CERES) program (Wielicki et al. 1995; Wielicki et al. 1996), which consists of earth radiation budget instrument packages flying on three satellites beginning with the Tropical Rainfall Measuring Mission (TRMM) satellite in late 1997 (Simpson et al. 1988), EOS-AM (Earth Observing System, 1030 LT sun-synchronous orbit) satellite in June 1998, and EOS-PM satellite in 2000 (1330 LT sun-synchronous orbit). Building on the successful Earth Radiation Budget Experiment (ERBE) program (Barkstrom 1984; Barkstrom et al. 1989), this three-satellite mission will provide the scientific community with the necessary information for monitoring the earth's radiation environment well into the next century. Plans are to deploy the CERES instruments in a three-satellite configuration over the 18-yr period. The three satellite configuration includes 1030 and 1330 LT sun-synchronous orbits plus one precessing orbit in order to sample the diurnal cycle of radiation.

The CERES instrument package is designed to measure the total (0.2–200 μm), shortwave (0.3–5.0 μm), and longwave window (8–12 μm) radiation from the earth using either the cross-track/bidirectional fixed azimuth scan mode or the rotating azimuth plane configuration (Lee et al. 1996; Wielicki et al. 1996). In the cross-track fixed azimuth scan mode, the detectors scan perpendicular to the spacecraft orbit plane in a whisk-broom fashion to collect radiation measurements. These measurements are the primary source of data used to monitor the radiation budget of the earth's system. The rotating azimuth plane scanning (RAPS) mode, on the other hand, will measure radiances from all geographical

Corresponding author address: Dr. Takmeng Wong, NASA/Langley Research Center, MS 420, Hampton, VA 23681-0001.
E-mail: takmeng.wong@larc.nasa.gov

© 1997 American Meteorological Society

Unauthenticated | Downloaded 11/11/24 08:52 PM UTC

scenes with varying incident solar radiation and observing geometry. The resultant angular radiance measurements will be used to construct new and improved angular dependence models (ADMs) for use in converting radiance measurements to flux estimates. The current CERES operational plan at the writing of this paper calls for two CERES instruments aboard both the EOS-AM and the EOS-PM spacecraft. One instrument will be operated in a cross-track scan configuration and the other in the rotating azimuth plane mode. The TRMM spacecraft will, however, have only one CERES instrument. It will operate in a cyclical fashion between the cross-track and the rotating angular scan modes to obtain both types of radiation measurements.

The TRMM CERES cross-track scanner data are the most important scientific measurements of the CERES program. To minimize the errors in the monthly mean radiation field due to missing CERES cross-track measurements during the RAPS mode period, the optimal sequence for cycling between the two scan mode configurations must be determined before launch. In this paper, analyses of the computer-simulated cross-track scanner data under various scan mode combinations are used to determine this optimal pattern. Section 2 gives an overview of the data used in this study and the method used in simulating the cross-track scanner dataset under different scan mode combinations. Error analyses of the monthly mean radiation fields for both the all-sky and the clear-sky simulations are presented in sections 3 and 4, respectively. Section 5 provides a summary of the conclusions for this study.

2. Data simulations

The data used for this study are from the ERBE S-4 daily mean cross-track scanner data product. This dataset contains 2.5° × 2.5° grid boxes of daily mean values of the TOA emitted longwave and reflected shortwave for both all-sky and clear-sky conditions. In addition, the ERBE S-4 clear-sky longwave daily mean data are limited only to oceanic regions. For this study, only the data derived from the Earth Radiation Budget Satellite (ERBS) in a region between 50°N and 50°S are considered. This dataset (hereafter referred as the truth dataset) is used to simulate other scanner datasets under different scan mode sequences (hereafter referred as the simulated data). In addition, data from three seasonal months (April 1985, July 1985, and January 1986) are also examined in this study in order to identify expected ranges of seasonal error in the resultant cross-track data.

A simple temporal sampling technique is used to simulate the scanner data collected during the different scan mode sequences. Specifically, this temporal sampling scheme is given by

$$X_{\text{stimulated}}(i, j) = \begin{cases} X_{\text{truth}}(i, j), & \text{if cross-track scanner is on,} \\ \text{undefined}, & \text{otherwise,} \end{cases} \quad (1)$$

TABLE 1. Scanner operation scenarios for the simulations.

Case	Cross-track scanner sequences		Observation days per month	
	Days on	Days off	Cross-track scanner	Rotating scanner
I	2	1	20	10
II	1	1	15	15
III	1	2	10	20
IV	20	10	20	10
V	15	15	15	15

where i is the 2.5° × 2.5° grid box region index and j is the day index within any 1-month period. Given the sequence scan mode operation, this sampling scheme will produce a dataset that imitates the daily mean radiation data collected from the cross-track scanner during the TRMM mission. For the current study, five scenarios, which are designated by the number of days in which the scanner is turned on and the number of days in which the scanner is turned off (i.e., the rotating azimuth scanner mode is turned on), are considered. Details of these cases are outlined in Table 1. The first and the fourth cases allow 20 days of cross-track scanner measurement and 10 days of rotating azimuth data per month. The second and the fifth cases have an equal number of observation days per month for each of the scan mode configurations. The third case is the opposite of the first.

The first step in the data analyses is to calculate monthly mean fields from the six datasets (one truth and five simulated sets) using a monthly averaging procedure,

$$\bar{X}(i) = \frac{\sum_j X(i, j)}{N(i)}, \quad (2)$$

where N is the total number of daily scanner measurements per month in any 2.5° × 2.5° grid region i. This procedure ignores any undefined data points in the set. Standard error analyses, including mean, standard deviation, and root-mean-square are then performed for each of the five simulated datasets to determine the optimal scan mode sequences for the TRMM single CERES instrument. For a particular simulated dataset, the monthly mean error over a specific 2.5° × 2.5° region i is defined as

$$\text{error}(i) = \bar{X}_{\text{simulated}}(i) - \bar{X}_{\text{truth}}(i), \quad (3)$$

where a positive error indicates an overestimation and a negative error suggests an underestimation.

3. All-sky results

The monthly mean all-sky longwave (LW) and shortwave (SW) radiation errors for the five scenarios in an area around the globe between 50°N and 50°S are shown in Tables 2 and 3, respectively. These errors are reported

Unauthenticated | Downloaded 11/11/24 08:52 PM UTC

TABLE 2. All-sky longwave errors (W m^{-2}).

	April 1985			July 1985			January 1986		
Case	Mean	SD	rms	Mean	SD	rms	Mean	SD	rms
I	0.0	2.3	2.3	0.1	2.0	2.0	0.1	2.0	2.0
II	0.0	2.4	2.4	0.1	2.1	2.1	0.0	2.0	2.0
III	−0.2	4.6	4.6	0.1	4.2	4.2	0.3	4.2	4.2
IV	−0.3	7.5	7.5	−0.6	5.2	5.2	−0.2	5.8	5.8
V	−0.3	10.7	10.7	−0.3	7.8	7.8	0.1	9.0	9.0

TABLE 3. All-sky shortwave errors (W m^{-2}).

	April 1985			July 1985			January 1986		
Case	Mean	SD	rms	Mean	SD	rms	Mean	SD	rms
I	−0.1	4.6	4.6	0.1	4.4	4.4	−0.1	4.7	4.7
II	−0.1	6.0	6.0	0.0	5.2	5.2	0.1	5.9	5.9
III	0.1	9.3	9.3	0.3	8.3	8.3	−0.1	9.4	9.4
IV	0.2	9.8	9.8	0.5	7.9	7.9	−0.1	9.3	9.3
V	0.1	13.5	13.5	0.1	11.1	11.1	−0.2	13.0	13.0

in terms of their mean (i.e., bias error), standard deviation (i.e., random error), and their associated root-mean-square (rms) error (i.e., total error) for all three seasonal months in the study. Four characteristics of these simulations are readily available from these two tables. These features are explained in more detail below.

First, the bias error for all the all-sky cases (SW and LW) is very close to zero, indicating that most of the total errors in these fields are due to random errors. For example, the LW and SW bias error for all 30 sets of calculations in this study never exceeds 0.6 W m^{-2}. Furthermore, there is no observable trend in the bias error as a function of the sampling strategy used. The random errors, on the other hand, depend strongly on sampling strategy and can reach values as large as 13.5 W m^{-2}. Therefore, the changes in the random error fields among different simulations dominate our current error analyses.

Second, the random error for each of the five scenarios increases with increasing number of consecutive days without cross-track scanner data. For example, the smallest random error is found in the first simulation with one day of missing cross-track data in every 3-day period of data collection. The largest random error is found in the last case with 15 consecutive days of missing cross-track data in every 30-day period. To better understand the cause of this behavior, the monthly mean LW regional error field for all five scenarios along with the truth monthly mean LW field for April 1985 are plotted on a global map in Fig. 1. For this period, the truth LW dataset (shown in Fig. 1a) displays a typical pattern of poleward decrease in LW radiation, corresponding to the poleward decrease in both temperature and moisture, with a range between 180 (the green regions) to 320 W m^{-2} (the purple area). Significant longitudinal variations in emitted LW radiation also exist and are indicative of the presence of deep convective clouds (i.e., regions over Indonesia, South America, and Central Africa). The global map for the monthly mean TOA LW error for each of the 2.5° × 2.5° grid boxes during April 1985 is shown in Figs. 1b–f for case I to case V, respectively. The color scale for this analysis ranges from purple for positive errors (overestimation) to dark blue for negative errors (underestimation). It is evident from this figure that regions of positive and negative errors are scattered over each field in a random fashion. Averaging over the entire globe, these regional errors tend to cancel, resulting in a very small global bias error for each of the simulations. It is also apparent that the LW all-sky error increases with the number of the days when the scanner is turned off. For example, the regions of dark blue (large negative error) and light pink (large positive error) increase in size as one moves from the first simulation (Fig. 1b) to the last simulation (Fig. 1f). The maximum LW error for the first simulation (2 days on and 1 day off) is 9.0 W m^{-2}, while it is 46.1 W m^{-2} for the last simulation (15 days on and 15 days off). From the above information, it is deduced that the increases in random error shown in Tables 2 and 3 are caused by the increasing magnitudes of regional error in these simulations. These regional errors are due to the inability of the simulations to capture the changes in the underlying cloudiness, meteorological, and surface conditions as the period of consecutive days of missing scanner data increases. For example, the background cloud conditions in the last simulation can change significantly over the 15 consecutive days when no cross-track scanner data are obtained. This missing information can translate into large regional errors (or random errors) in the final monthly radiation fields. The results in Fig. 1 are consistent with earlier statistical studies of outgoing longwave radiation (OLR) by Cahalan et al. (1982) and Charlock et al. (1988). Using the daily variations in OLR as a proxy for changes in cloudiness, Cahalan et al. (1982) found that the characteristic timescale for day-to-day regional fluctuations in cloudiness is on the order of 2 days and less. Thus, in order to minimize the effects of these cloudiness changes on the monthly mean radiation fields, the observed timescale in regional cloudiness fluctuations must be properly resolved by the temporal sampling strategy of the instrument. Hence, a temporal sampling strategy with more than 1 day of missing cross-track scanner measurements will produce large regional errors in the monthly mean radiation fields.

Third, the SW random errors are always larger than the LW errors. For example, the SW error in Table 3 is often twice as large as its LW counterpart. This is due mainly to the fact that the influences of cloud systems are much larger at solar wavelengths than in the thermal infrared. Thus, the missing cross-track scanner data causes larger errors in the monthly mean SW fluxes. These differences decrease somewhat as the number of consecutive days without cross-track scanner data increases.

Unauthenticated | Downloaded 11/11/24 08:52 PM UTC

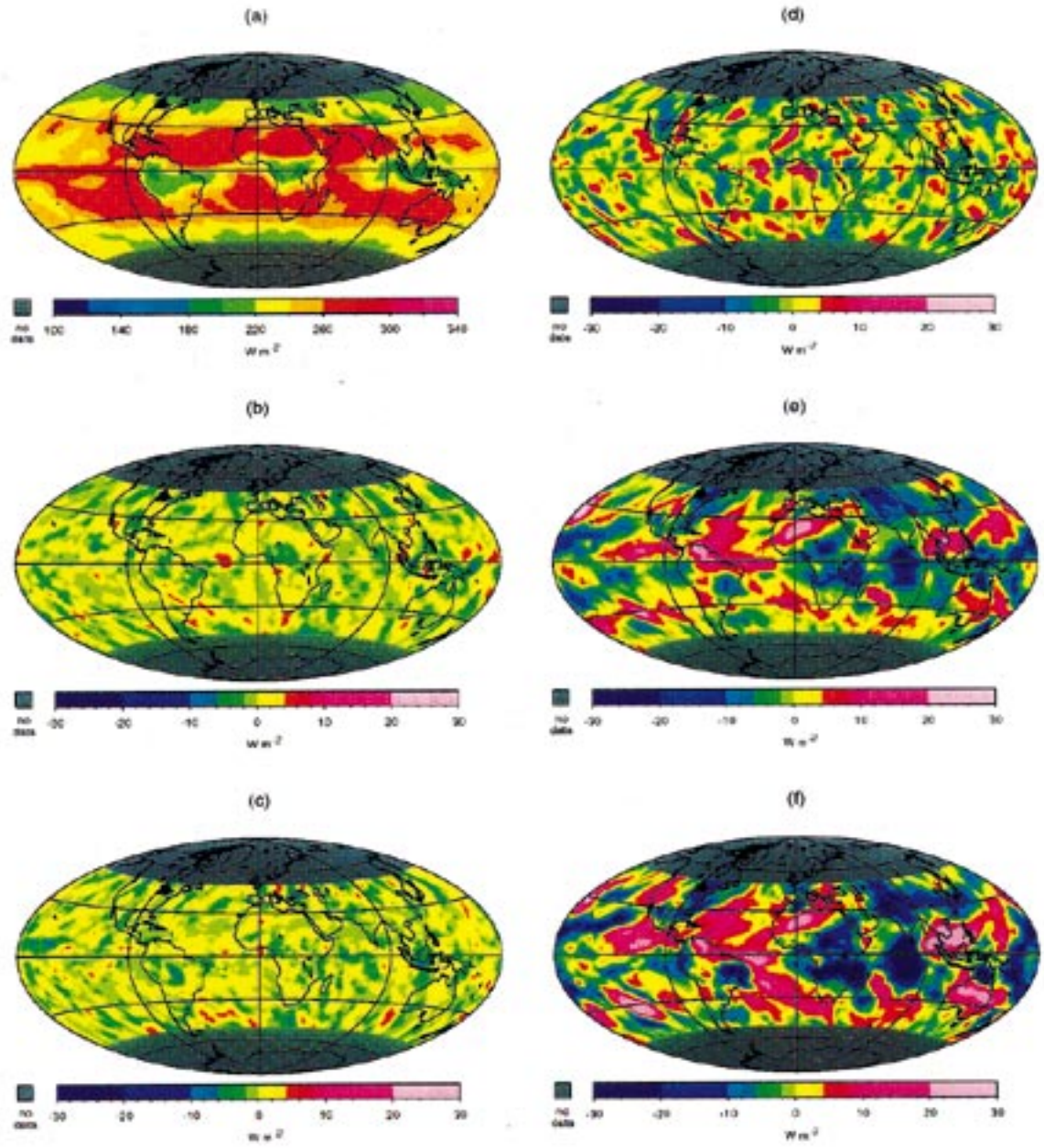

FIG. 1. The monthly mean all-sky regional scale (a) outgoing longwave radiation field in watts per square meter derived from ERBS 2.5° scanner data for April 1985 and the simulated monthly mean all-sky regional scale longwave radiation error (simulation minus truth) in watts per square meter for (b) 2 days on 1 day off, (c) 1 day on 1 day off, (d) 1 day on 2 days off, (e) 20 days on 10 days off, and (f) 15 days on 15 days off.

Fourth, the bias errors in both longwave and shortwave radiation have very little seasonal dependence (i.e., less than 0.6 W m^{-2} for the worst case). The random error field, however, has a larger seasonal variation. To illustrate this point more clearly, the bias error and the random error for each of the 3 months and each of the five cases are plotted in Fig. 2. The seasonal dependence of the bias errors is very small for all five simulations. Seasonal dependence of the random errors is small ($<$0.8 W m^{-2}) for the first two simulations, but larger variations are noted for case III to case V simulations. These seasonal changes, however, do not exceed 3.5 W m^{-2} for the worst cases.

From these analyses, it is determined that the ''2 days on 1 day off'' case is the optimal scan mode sequence for minimizing total errors in the monthly mean all-sky

Unauthenticated | Downloaded 11/11/24 08:52 PM UTC

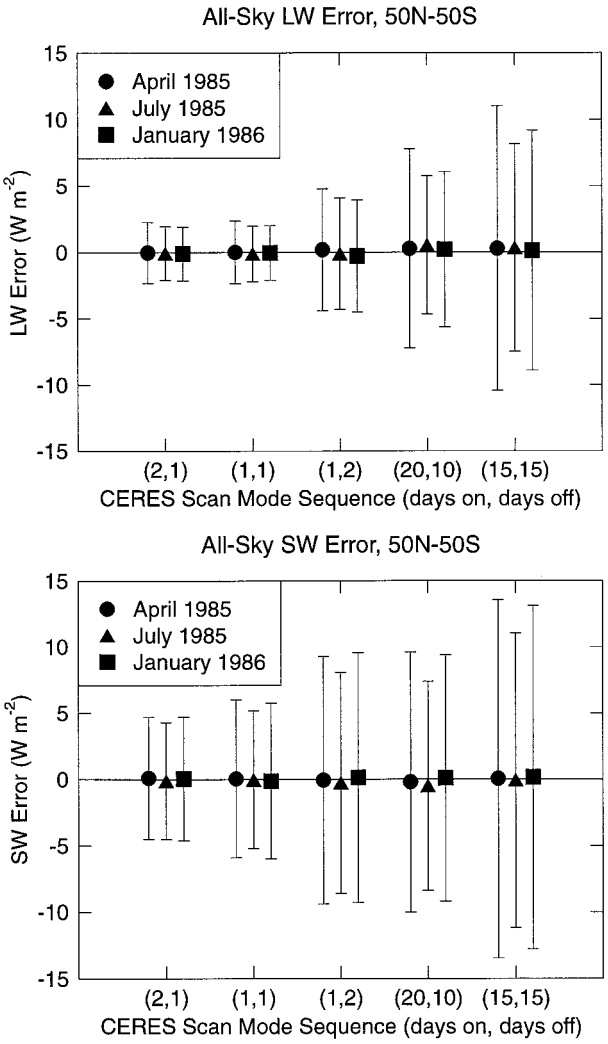

FIG. 2. The simulated monthly mean all-sky longwave (top) and shortwave (bottom) bias error (markers) in watts per square meter and random error (given by plus and minus one standard derivation of the data and shown in bar) as a function of the CERES scan mode sequence [(2, 1) for 2 days on 1 day off; (1, 1) for 1 day on 1 day off; . . . , (15, 15) for 15 days on 15 days off], and season (solid circle for April 1985; solid triangle for July 1985; solid square for January 1986).

longwave and shortwave radiation field. Furthermore, this case also has the smallest seasonal variation in total error. The rms error on the monthly mean all-sky fields for this case is expected to be less than 2.5 W m^{-2} for LW and 5.0 W m^{-2} for SW measurements. The seasonal variations in all-sky total error for this simulation are less than 0.3 W m^{-2}.

4. Clear-sky results

Error analyses for the same scenarios under clear-sky conditions were carried out for April and October 1985 and January 1986. These results are given in Tables 4 and 5. Comparisons among these tables and Tables 2 and 3 suggest that the basic characteristics of the clear-sky simulations are very similar to their all-sky counterparts. Some small differences are also noted in these comparisons as outlined below.

TABLE 4. Clear-sky longwave errors (W m^{-2}).

	April 1985			July 1985			January 1986		
Case	Mean	SD	rms	Mean	SD	rms	Mean	SD	rms
I	0.0	0.3	0.3	0.0	0.3	0.3	0.0	0.3	0.3
II	0.0	0.3	0.3	0.0	0.3	0.3	0.0	0.3	0.3
III	0.0	0.7	0.7	0.0	0.6	0.6	0.0	0.6	0.6
IV	0.5	2.2	2.3	−0.5	1.7	1.8	0.1	1.8	1.8
V	0.6	3.1	3.2	−0.8	2.5	2.6	−0.1	2.6	2.6

The bias errors for all five clear-sky cases (SW and LW) are again very close to zero, indicating that the sampling errors are random, as expected. The random errors for each of the five scenarios also increase with increasing number of consecutive days without cross-track scanner data. Unlike the all-sky results, the smallest total LW clear-sky error is found in the second simulation. The differences in total LW errors between the first and the second scenario are, however, very small (i.e., less than 0.1 W m^{-2}). Thus, one can assume that LW clear-sky results are identical between these two simulations.

The clear-sky random errors are significantly smaller than their all-sky counterparts. For example, the maximum longwave (shortwave) regional error for the first all-sky simulation (i.e, ''2 days on and 1 day off'' case) is 8.9 (21.9) W m^{-2}, while it is 1.6 (17.7) W m^{-2} for the clear-sky case. Unlike the all-sky results, the regional errors in the clear-sky results are not caused by changes in cloudiness, but are due solely to variations in the background meteorological and surface conditions.

Similar to the all-sky results, the SW clear-sky total errors are larger than their LW counterparts. While the bias errors in LW clear-sky radiation fields for the first three simulations show very little seasonal dependence, much larger variations in seasonal bias errors are found in the remaining simulations. The SW clear-sky results, on the other hand, do not show any preferred seasonal pattern. To illustrate this point more clearly, the bias error and the random error for each of the 3 months and each of the five cases are plotted in Fig. 3. The scale on the figure has been reduced with respect to Fig. 2 to

TABLE 5. Clear-sky shortwave errors (W m^{-2}).

	April 1985			July 1985			January 1986		
Case	Mean	SD	rms	Mean	SD	rms	Mean	SD	rms
I	−0.1	1.5	1.5	0.0	1.5	1.5	0.0	1.5	1.5
II	0.0	1.7	1.7	0.1	1.7	1.7	0.0	1.7	1.7
III	0.1	2.7	2.7	0.0	2.5	2.5	0.0	2.6	2.6
IV	0.1	2.1	2.1	0.0	1.8	1.8	−0.1	2.0	2.0
V	0.0	3.0	3.0	−0.1	2.4	2.4	−0.1	2.6	2.6

Unauthenticated | Downloaded 11/11/24 08:52 PM UTC

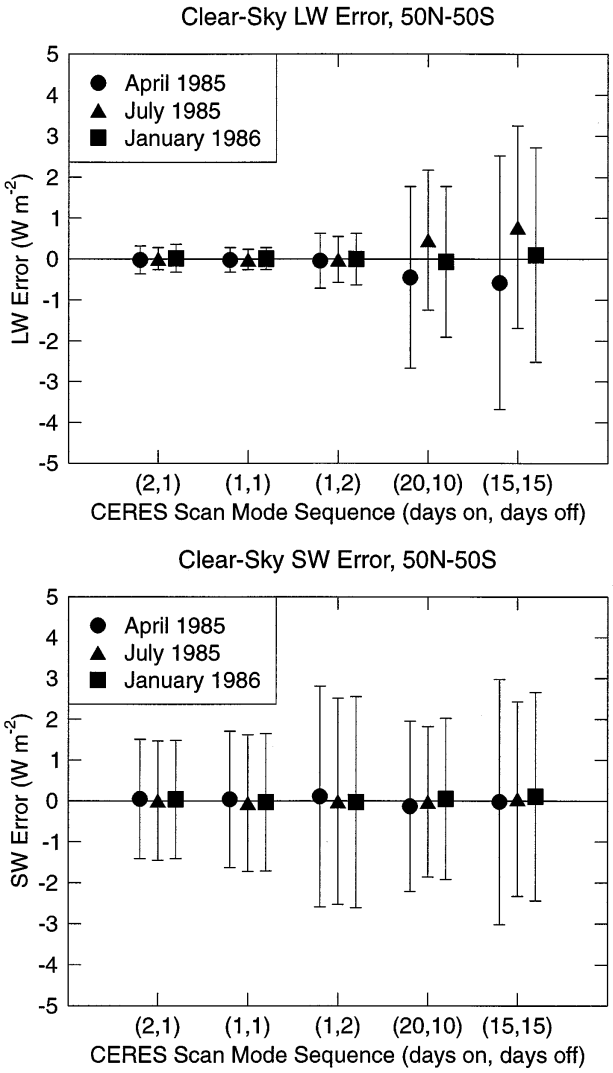

FIG. 3. Same as in Fig. 2 but for clear-sky conditions.

better show the smaller clear-sky errors. It is clear from this figure that there is a shape change in the seasonal dependence of the LW bias errors as one moves from the first three scenarios to the fourth and the fifth simulations. The largest seasonal change in LW bias errors in these simulations is less than 1.5 W m^{-2} and is due to changes in seasonal temperature and moisture profiles of the atmosphere.

From these analyses, it is again determined that the first scenario is the optimal scan mode sequence for minimizing total errors in the monthly mean clear-sky LW and SW radiation fields. The rms error on the monthly mean clear-sky radiation field for this case is expected to be less than 0.5 W m^{-2} for LW and 1.5 W m^{-2} for SW measurements. The seasonal variation in clear-sky total error for this simulation is less than 0.1 W m^{-2}.

5. Summary and conclusions

With the launch of the TRMM spacecraft in late 1997, CERES will begin to provide detailed long-term radiation budget measurements of the earth–atmosphere system. The single CERES instrument onboard the TRMM satellite is designed to be operated in either the traditional cross-track scan mode or a new RAPS configuration. While the RAPS configuration is used for improving current ADMs, the cross-track scan mode is the primary data source for monitoring the earth's radiation budget. For the TRMM mission, the single CERES instrument is required to collect both types of measurements. To minimize the errors in the derived monthly mean radiation fields caused by missing cross-track scanner data, an optimal sequence for cycling between these two scan mode configurations must be used to obtain the desired radiation measurements. This paper has presented analyses of monthly mean scanner data under simulated observing conditions to determine this optimal pattern.

Using the ERBE S-4 daily mean cross-track scanner dataset for April and July 1985 and January 1986 and a simple temporal sampling scheme to simulate the daily mean cross-track scanner data collected during the different scan mode sequences, five sets of simulated data were produced. Error analyses were performed on monthly mean radiation fields derived from these simulated cross-track scanner datasets. Five characteristics of the error field are identified from these analyses. While the global bias errors of these simulations are close to zero, significant regional/random errors exist for each individual case. These regional errors are caused by the inability of the simulations to capture the underlying changes in the cloudiness, meteorological, and surface conditions as the number of consecutive days with missing data increases. The SW total errors are always larger than the LW errors. The clear-sky total errors are always smaller than the all-sky errors. Furthermore, the seasonal variations in total errors are small in most cases.

It is concluded from the intercomparison among these five scenarios that the best results are obtained when the cross-track scanner is operated on a ''2 days on and 1 day off'' mode. This scan mode sequence will effectively allow for 2 consecutive days of cross-track scanner data and 1 day of angular radiance measurements for each 3-day period. The rms error on the monthly mean fields for this configuration is less than 2.5 W m^{-2} for the all-sky LW, 5.0 W m^{-2} for the all-sky SW, 0.5 W m^{-2} for clear-sky LW, and 1.5 W m^{-2} for SW clear-sky measurement. These new radiation data should provide the scientists with improved tools for understanding the nature of the earth's climate and climate change.

Acknowledgments. The authors wish to thank Dr. Bruce Wielicki of the NASA Langley Research Center

Unauthenticated | Downloaded 11/11/24 08:52 PM UTC

and an anonymous reviewer for their constructive comments and suggestions.

REFERENCES

Barkstrom, B. R., 1984: The Earth Radiation Budget Experiment (ERBE). *Bull. Amer. Meteor. Soc.,* **65,** 1170–1185.

——, E. F. Harrison, G. L. Smith, R. N. Green, J. Kibler, R. Cess, and the ERBE Science Team, 1989: Earth Radiation Budget Experiment (ERBE) archival and April 1985 results. *Bull. Amer. Meteor. Soc.,* **70,** 1254–1262.

Cahalan, R. F., D. A. Short, and G. R. North, 1982: Cloud fluctuation statistics. *Mon. Wea. Rev.,* **110,** 26–43.

Charlock, T. P., K. M. Cattany-Carnes, and F. Rose, 1988: Fluctuation statistics of outgoing longwave radiation in a general circulation model and in satellite data. *Mon. Wea. Rev.,* **116,** 1540–1554.

Lee, R. B., III, and Coauthors, 1996: The Clouds and the Earth's Radiant Energy System (CERES) sensors and preflight calibration plans. *J. Atmos. Oceanic Technol.,* **13,** 300–313.

Simpson, J., R. F. Adler, and G. R. North, 1988: A proposed Tropical Rainfall Measuring Mission (TRMM) satellite. *Bull. Amer. Meteor. Soc.,* **69,** 278–295.

Wielicki, B. A., R. D. Cess, M. D. King, D. A. Randall, and E. F. Harrison, 1995: Mission to Planet Earth: Role of clouds and radiation in climate. *Bull. Amer. Meteor. Soc.,* **76,** 2125–2153.

——, B. R. Barkstrom, E. F. Harrison, R. B. Lee III, G. L. Smith, and J. E. Cooper, 1996: Clouds and the Earth's Radiant Energy System (CERES): An Earth Observing System Experiment. *Bull. Amer. Meteor. Soc.,* **77,** 853–868.

Unauthenticated | Downloaded 11/11/24 08:52 PM UTC